# Experiments in Splashing

by

Jameson Lawrence Toole

A thesis submitted in partial fulfillment
of the requirements for the degree of
Bachelor of Science: Honors Physics
(Department of Physics)
in The University of Michigan
2009

Thesis Committee:

Professor Robert Deegan, Advisor

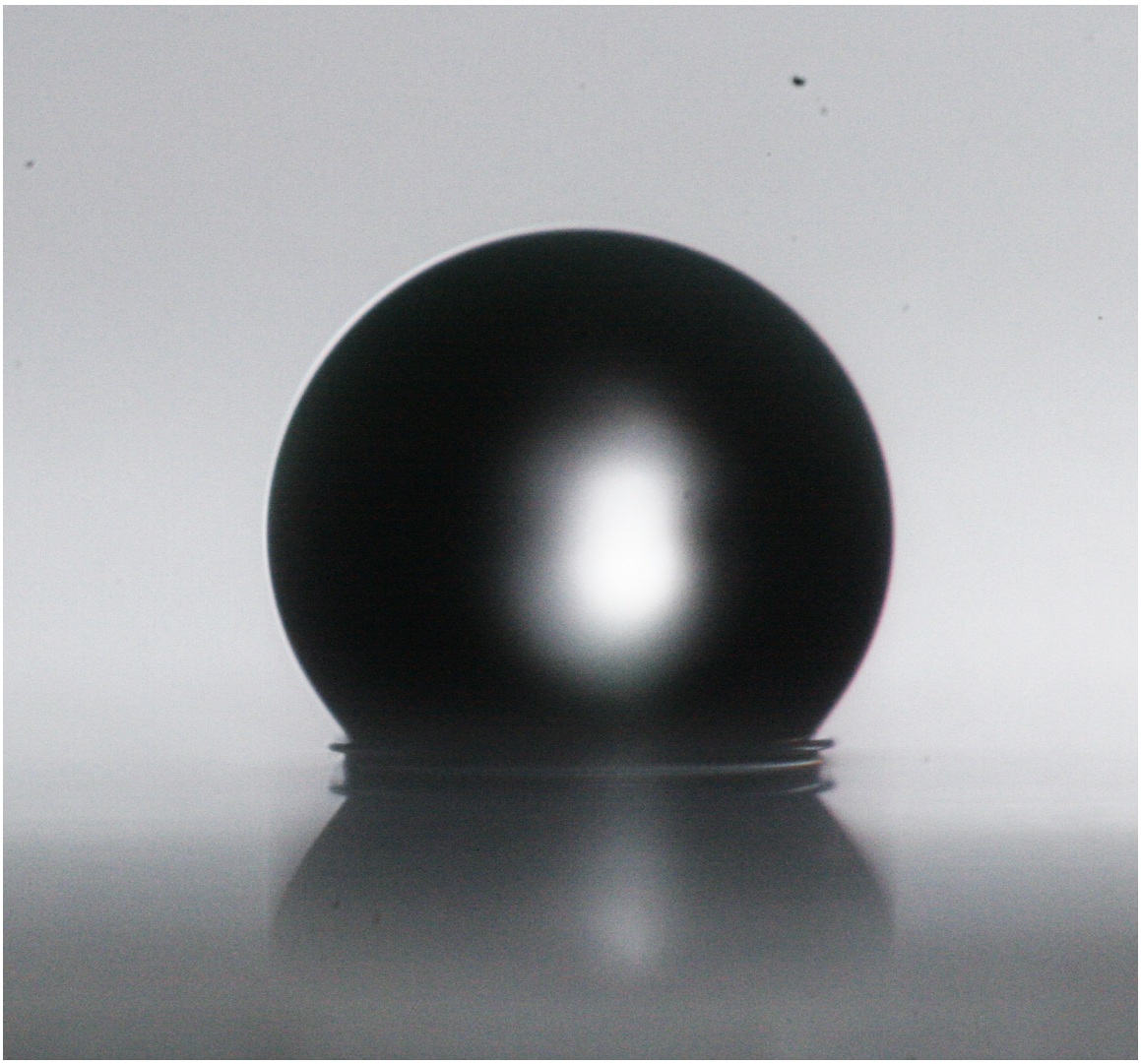

To the people who fill each day with things to learn and questions to ask.

# ACKNOWLEDGEMENTS

First and foremost, I would like to thank my advisor, Professor Robert Deegan, for his patience, guidance, and support in all aspects of this work. His willingness to accept the challenge of bringing a wide-eyed sophomore into his group was a remarkable display of kindness and ability. In addition, I would like to thank Tamir Epstein for his daily help and encouragement. His willingness to share advice and tricks of the trade has proved invaluable time and time again. Finally, I would like to thank my parents for supporting my access to such a wonderful environment to learn and grow.

# TABLE OF CONTENTS

# LIST OF FIGURES

**Figure**

# ABSTRACT

Experiments in Splashing
by
Jameson Lawrence Toole

Advisor: Robert Deegan

In this work we present a suite of experiments exploring the complexities of splashing. We begin by revealing discrepancies in the phase space of splashing parameters, followed by a brief clarification of the anatomy of a splash. Having established a universal language, we probe the origin and evolution of fluid sheets produced during a splash. We provide evidence that the characteristics of these sheets are responsible for qualitative features of the splash. Building on previous work, we then test the hypothesis that the composition of surrounding gas has a significant effect on splashing. Finally, we describe a series of miscellaneous experiments aimed at exploring novel combinations of parameters and initial conditions. From these experiments, we provide some evidence that both impacting drop and fluid layer contribute to the liquid sheets of a splash.

# CHAPTER I

# Introduction

> There will be but few of my readers who have not, in some heavy shower of rain, beguiled the tedium of enforced waiting by watching, perhaps half-unconsciously, the thousand little crystal fountains that start up from the surface of pool or river; noting now and then a surrounding coronet of lesser jets, or here and there a bubble that floats for a moment and then vanishes.
>
> *- A. M. Worthington [11]*

Though the fast eye of Da Vinci may have been the first to record the structure of a splash, it wasn't until the strobe photography of Worthington in the early 1900s that the complexities of splashing were systematically captured on film [11]. In a series of experiments using pioneering photographic techniques, Worthington characterized the splashing of liquid and solid objects into fluid. In addition to thorough categorization, his work also proposed explanations for many features of a splash.

While images of splashing remain a source of fascination and entertainment, broader applications include gas transfer to bodies of water, spray coating and printing, cooling, and even acoustic properties such as the underwater sound of rain [14]. Despite the wealth of possible applications, surprisingly few quantitative results have be produced. Thus, fundamental research is focused on identifying control parameters governing the dynamics of splashing.

In this work, we present a series of experiments designed to explore the phase space of splashing regimes as well as experimentally test several theories pertaining to various features of a splash. Specifically, we study the splashing of a small liquid drop onto a thin layer of fluid. Carefully controlling initial conditions and fluid properties, we use still and high speed video photography to capture splashes. Digital image processing techniques are then used to quantify the evolution of various parameters.

This research is partitioned into four related components: the examination of inconsistencies in the characterization of splashing by dimensionless quantities, the origin and evolution of fluid sheet(s) ejected during splashing, the influence of the surrounding gas on the two previous experiments, and finally miscellaneous observations and experiments.

# CHAPTER II

# Phase Portraits and Dynamic Similarity

## 2.1 Introduction

Dynamic similarity ensures that if specific relations between two systems are held constant, differences in the absolute parameters of each system will not affect observed dynamics. This law allows engineers to test model airplanes in a wind tunnel to expect full-scale versions to fly as well. Dynamic similarity is an extremely important concept for studying high-dimensional systems such as splashing, helping to greatly reduce the parameter space. It allows more flexible choices of materials, experimental apparatus, and procedures. In this chapter, we present new data suggesting the current set of dimensionless parameters are insufficient to fully characterize a splash.

## 2.2 Theoretical Background

For a liquid droplet splashing on a thin layer of fluid, the Navier-Stokes equations require the inclusion of seven parameters. Three of these describe the fluid ($\rho$ - density, $\gamma$ - surface tension, and $\nu$ - dynamic viscosity), while the remaining four specify the physical parameters of the system($D$ - diameter of the drop, $U$ - speed of the drop at impact, $h$ - depth of the layer, and $g$ - acceleration due to gravity).

From unit analysis, there are three fundamental quantities (time, length, and mass) that are combined to form each of the seven parameters. Subtracting the number of parameters from the number of fundamental quantities reveals four dimensionless quantities that can completely characterize the system. However, the specific combinations of the seven parameters forming the dimensionless quantities is not unique.

By convention, the four dimensionless numbers are specified as follows [2]:

$$Re = \frac{DU}{\nu},\ We = \frac{\rho DU^2}{\gamma},\ Fr = \frac{U^2}{gD},\ H = \frac{h}{D}. \tag{2.1}$$

The Reynolds number ($Re$) measures the ratio of inertial forces to viscous forces, while the Weber number ($We$) is a ratio of inertia to surface tension. Of the two other numbers, the Froude ($Fr$) number is a measure of the affects of gravity and is small enough to ignore in our experiments, and the dimensionless depth ($H$) is either kept constant at a value of $H = 0.2$ or not controlled for. Other combinations of these numbers sometimes include the Ohnesorge number ($Oh = \sqrt{We}/Re$).

Holding two of these numbers constant, we have narrowed the parameter space to two dimensions, $Re$ vs. $We$. By dynamic similarity, picking any two systems sharing a common Weber and Reynolds number should display the same characteristic splash. Early work by Stow and Hadfield found a splash/no-splash boundary in terms of these two numbers for liquid droplets impacting on dry solid surfaces [8], while later work by Cossali and Sommerfeld again phrased this boundary in terms of various dimensionless numbers [1], [6]. Similar relations have also been discovered in more complicated systems, such as the case where a stream of water droplets splashes on a solid surface [14].

Beyond the simple categorization of splash versus no-splash, Deegan *et. al.* have identified a number of splashing regimes in the two dimensional $Re$ vs. $We$ space [2]. Figure 2.1 shows four specific regions, no-splash, crown splash, microdoplet splash, and a combination with both the crown and microdroplet splash.

A non-splashing event is characterized by the droplet impacting on the layer of fluid, neither immediately ejecting smaller droplets nor producing a crown that breaks up after some time. A microdroplet splash is characterized by small secondary droplets are ejected from the impact site almost immediately, though the fluid sheet produced does not break up at a later time. A crown splash, on the other hand, does not produce any droplets after impact, but instead features a crown whose rim eventually becomes unstable, producing jets of secondary drops. Finally, a combination of the two is characterized by both microdroplets at impact as well as an unstable crown. A series of images corresponding to each of the types of splashes can be found in Figure 2.2

While a number of properties, including those of the fluid and the droplet, determine a location in the phase space, we are able to navigate by relating the Reynolds

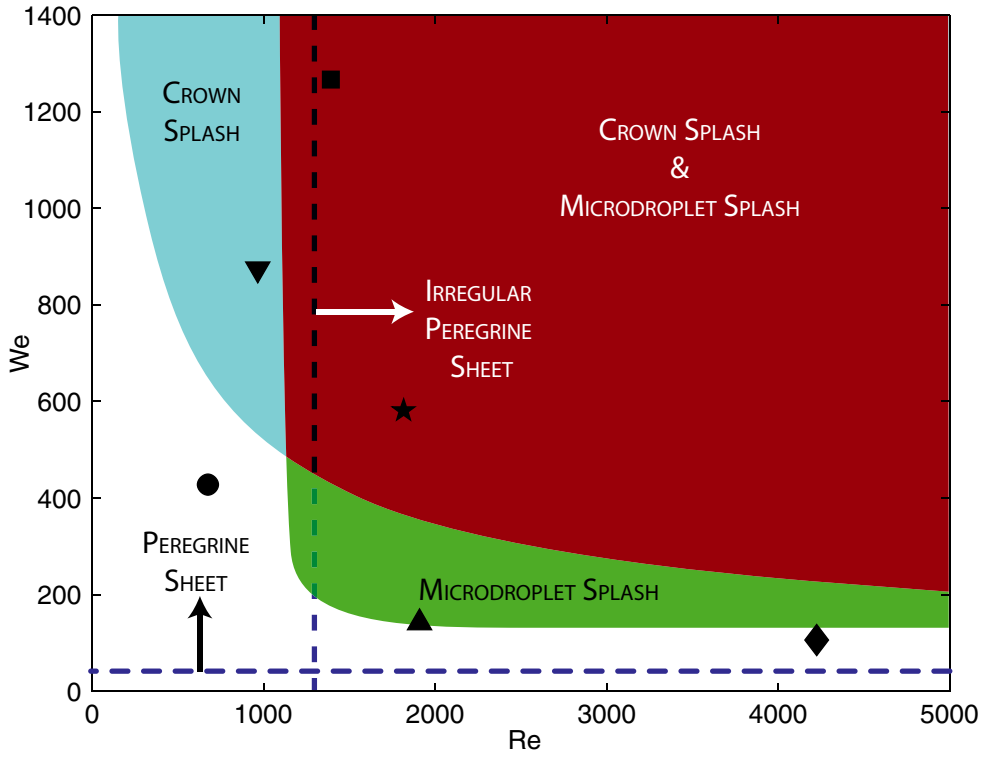


Figure 2.1: A phase portrait presented by Deegan *et. al.* displaying four splashing regimes characterized by the Reynolds and Weber numbers [2].

and Weber numbers in the following way:

$$We = \frac{\rho D U^2}{\gamma} = \frac{\nu^2 \rho}{\gamma D} Re(U)^2 \tag{2.2}$$

Choosing a single liquid, the fluid properties are held constant for all impacts involving the particular substrate. Next, we fix the drop diameter by careful experimental techniques outlined in later sections. Hence, each fluid has a corresponding curve through phase space and we can move along this curve by altering the impact speed of each droplet. We can now sweep the phase space by choosing a set of curves corresponding to fluids with different properties such as viscosity or density, and examine splashes along individual curves by altering impact speed. As an example, Figure 2.3 shows a set of curves for water-glycerol mixtures of different concentration as well as silicone oils of varying viscosity.

From the discussion of dynamic similarity in the beginning of this section, we note that if our system can be completely described by specifying these two dimensionless numbers (the other two are held constant), then, with careful choice of the drop diameter and impact speed, splashes on two overlapping curves will be exactly the

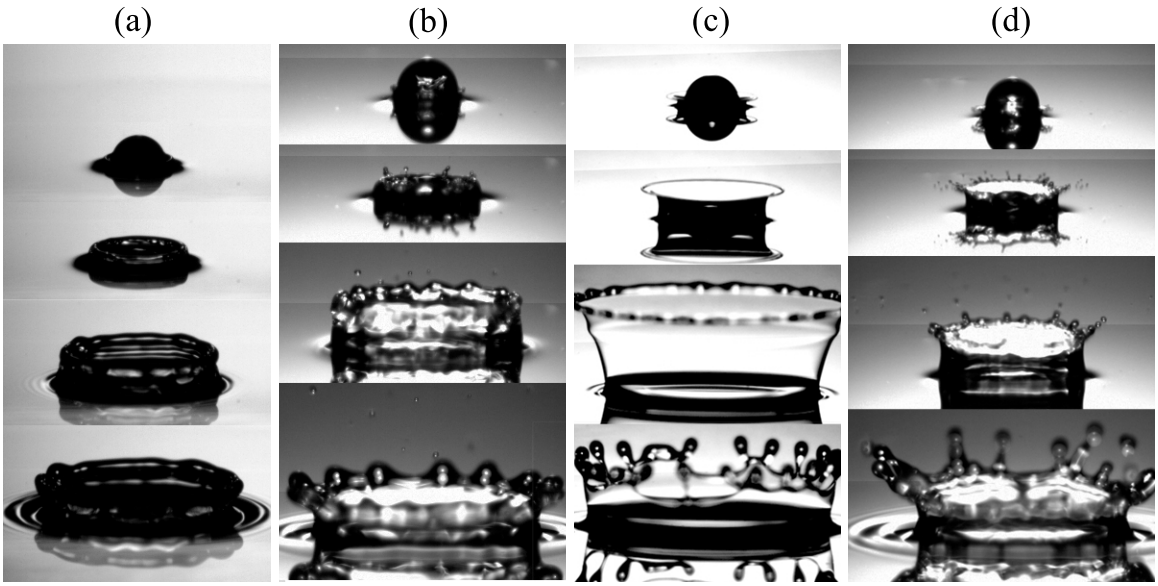


Figure 2.2: (a)No splash is produced by 0.65cSt silicone Oil impacting with $Re = 3600$ and $We = 184$. Images were recorded at, 427$\mu$s, 902$\mu$s, 2517$\mu$s, and 4227$\mu$s after impact. (b) A water droplet with $Re = 4000$ and $We = 157$ produces microdroplets. Images were recorded at 237$\mu$s, 617$\mu$s, 2185$\mu$s, and 4730$\mu$s after impact. (c) 5cSt silicone Oil splashing with $Re = 1000$ and $We = 1000$ produces a classic crown splash. Images taken at 202$\mu$s, 454$\mu$s, 2995$\mu$s, and 5445$\mu$s after impact. (d) A water drop impacting with $Re = 5000$ and $We = 260$ features both microdoplets and a crown splash. Images recorded at 143$\mu$s, 428$\mu$s, 1188$\mu$s, and 5938$\mu$s after impact.

same even if the fluids are different. In the following sections, we will provide evidence that these two numbers are not enough to fully describe each splash and that different fluids will produce two distinctly different splashes despite their close proximity in phase space.

## 2.3 Apparatus and Procedure

A diagram of the experimental apparatus can be found in Figure 2.4. Videos of splashes were recorded using a Phantom v7 high-speed camera coupled with a Nikkor 105mm macro-lens. Using a 500W halogen lamp to illuminate the falling drops, images could be recorded up to $100,000$fps, though in most cases $20,000$fps provided sufficient time resolution. For each splash, a series of $512 \times 256$ images were taken from these video files.

Drops were produced by a gravity reservoir that fed into a hollow, beveled needle.

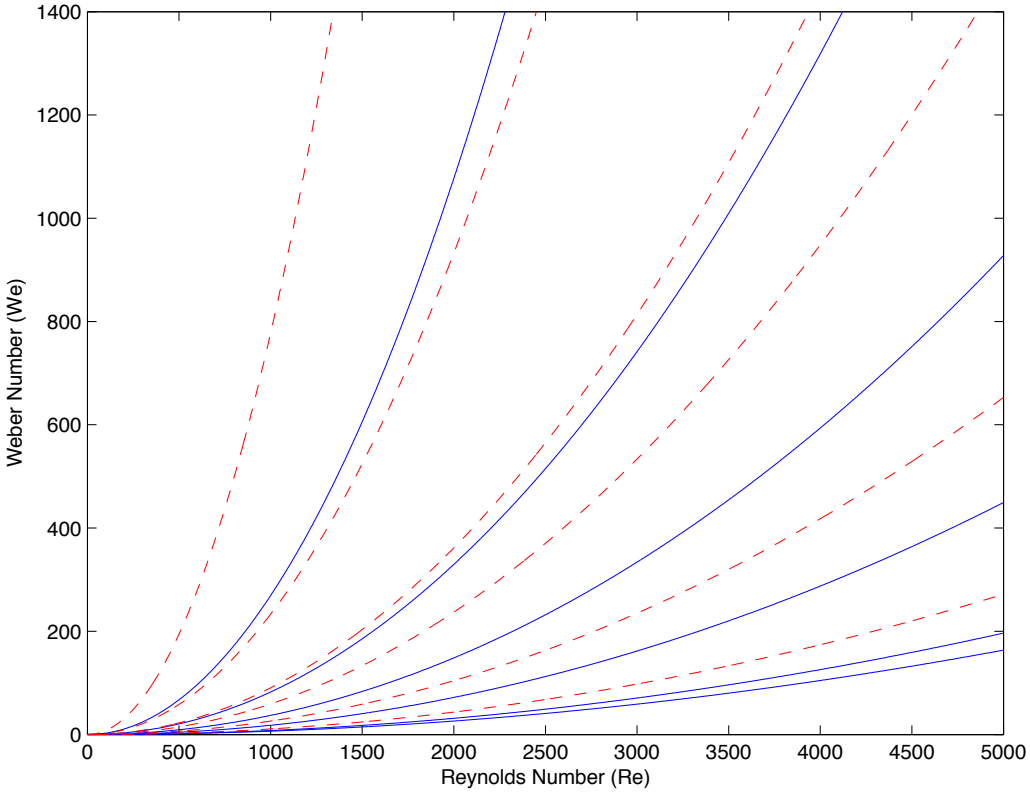


Figure 2.3: A systematic sweeping of the phase space involves choosing a set of fluid curves and examining splashing along them. The blue (solid) curves represent water and glycerol mixtures of varying concentration. The curves closer to the bottom right corner have higher percentages, by weight, of water. The red (dashed) curves correspond to silicone oils with differing viscosities (and density). Curves closer to the top left have higher viscosity.

This method produced drops with uniform diameter and control over the time between drops by changing the amount of fluid in the reservoir. Different drop sizes were achieved by using different sized needles. For most fluids, drops between 1.5 and 2.5 mm were produced. In addition to generating uniform drops, the beveled portion of the needle ensured that each drop began its fall with the same initial conditions and would impact within the very small area (only a few millimeters in radius) in front of the high-magnification camera lens.

Splashes occurred on a liquid layer placed below the needle. To ensure drops splashed on a uniform, thin layer of fluid, an optical flat (flat to within $\frac{\lambda}{4}$) was set on a kinematic mount and submerged in the liquid reservoir. The height of the flat was then adjusted to control the thickness of the coating on top of the glass. Before the optical flat was coated, however, a laser was used to level its surface. This was done

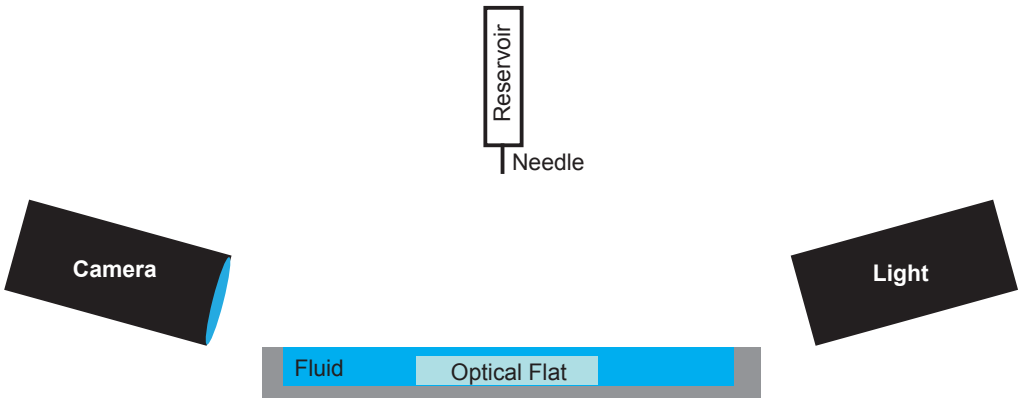


Figure 2.4: Apparatus for collecting phase space data.

by shining a beam perpendicular to the flat then adjusting the kinematic mount until the beam's reflection retraced its incoming path exactly. Using this method, we were able to ensure the optical flat was level to within $10^{-3}$ radians.

With the optical glass leveled and submerged, the layer thickness was measured with a needle and digital micrometer. The caliper was zeroed where the point of the needle contacted the fluid surface. The needle was then lowered into the fluid until it contacted the optical flat. In this way, we were able to measure the layer thickness to within $10\mu$m. To keep the dimensionless depth, $H = 0.2$ constant, layer thicknesses between 250 and $400\mu$m were used depending on specific drop diameters. The layer thickness was tested and adjusted regularly to control for evaporation and build up from previous drops.

Data was taken for a variety of fluids. For each specific liquid, the drop diameter (determined by needle size) was used to set the layer the depth. The gravity fed drop reservoir was filled so that the time between drops was approximately 10s, allowing the thin layer to relax after each splash. To achieve variety in impact speed, we varied the initial height of each drop, setting the tip of the needle within a range of $5 - 100$cm above the liquid surface. At each height, multiple splashes were recorded to verify repeatability.

From each video recording a length scale was calibrated by capturing an image of a ruler. Frame-by-frame analysis was then used to determine the exact time and drop speed of impact. Corrections were also made, considering the viewing angle of the camera. With the starting frame and exposure time known, the evolution of each splash could then be time stamped. We used this procedure to systematically study splashes for a range of fluids and impact speeds.

## 2.4 Results

Two fluids were chosen, 0.65cSt silicone oil and a Water-Glycerol mixture. The concentration of latter was kept at 90.4% water and 9.6% glycerol so that drops from both fluids could share $Re$ and $We$ numbers. Because of differences in the liquid properties the heights at which the numbers match are not the same. The water-glycerol drops were released significantly higher (from $10 - 60$cm) than the silicone oil ($7 - 36$cm).

For each fluid, a series of splashes with different impact speeds (drop heights) was recorded. The video files were converted to image sequences and the speed of each impact recorded. With this data, we calculated the Reynolds and Weber numbers of each splash. The videos were then examined for qualitative differences. Plots of these splashes in phase space can be found in Figure 2.5.

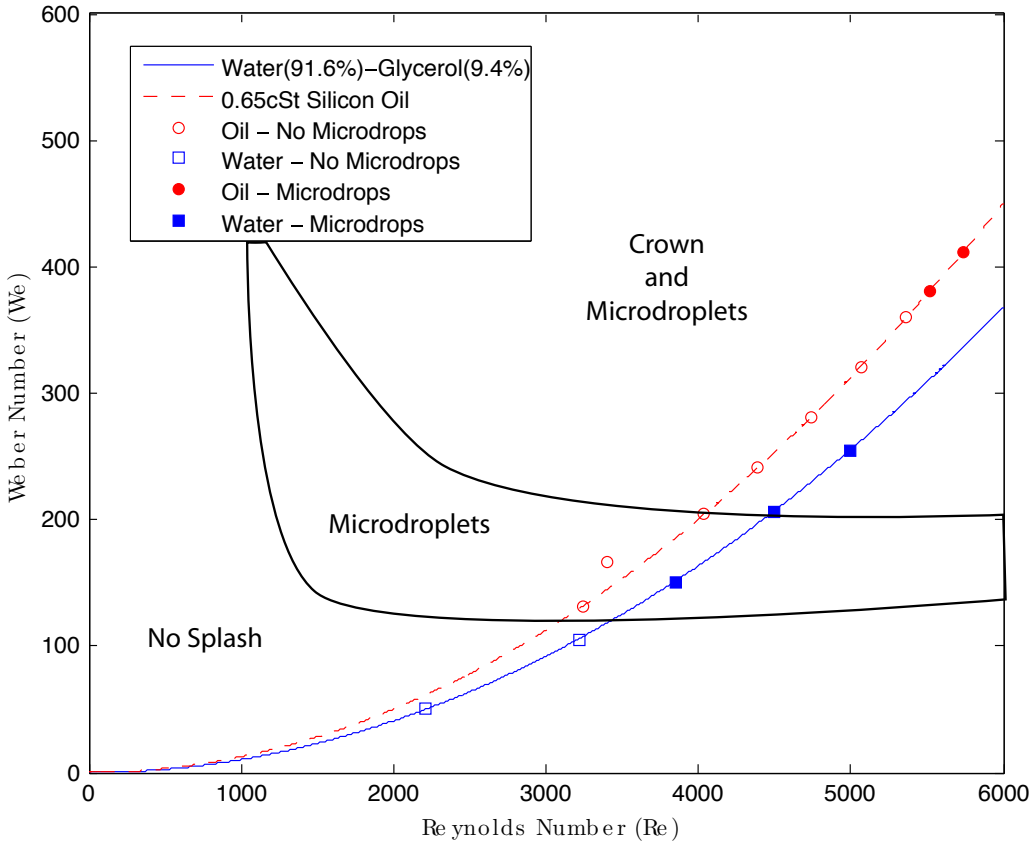


Figure 2.5: Splashes are recorded for two fluids. Though the splashes are close in the phase portrait, they display very different characteristics. The red (dashed) line is 0.65cSt silicone Oil, which only produced microdroplets for $Re > 5500$, while the blue (solid) curve represents a Water-Glycerol mixture that displayed microdrop splashes for $Re > 3700$.

We then selected two splashes, one for each liquid, whose $Re$ and $We$ numbers differed by less than 10%. We found that despite the close proximity in the phase space and the points position in previously explored splashing regimes, the splashes differed significantly. For example, silicone oil drops with $Re = 4043$ and $We = 206$ did not generate any microdroplets and produced a smooth liquid sheet, in stark contrast to water-glycerol drops with $Re = 4498$ and $We = 204$ which produced microdroplets and had an unstable sheet. Despite the $Re$ and $We$ numbers of the water-glycerol drops differing from the oil by 10.1% and 1.0%, respectively, obvious differences were found. Images of these two splashes can be found in Figure 2.6.

More generally, we found microdroplets were generated by water-glycerol drops for splashes with $Re > 3700$ and $We > 150$. The no-splash/microdroplet boundary for silicone oil did not occur until much higher numbers were attained, $Re > 5500$ and $We > 350$. When this boundary was reached, however, comparing two splashes that both produce microdrops (even for different fluids and $Re$ and $We$ numbers) reveals expected similarities. Figure 2.7 shows an oil drop producing microdroplets for $Re = 5739$ and $We = 412$. It is qualitatively similar to the water-glycerol splash seen above, despite their distance in phase space.

## 2.5 Conclusion

Discrepancies found in splashing regimes of different liquids lead us to conclude that our attempt to describe a splash by specification of the four dimensionless numbers defined is insufficient. We have shown that two drops may produce qualitatively different splashes, despite having nearly identical dimensionless parameters as described by Equation 2.1. These results suggest that the parameter space being considered, namely the high Reynolds number regime, is incomplete.

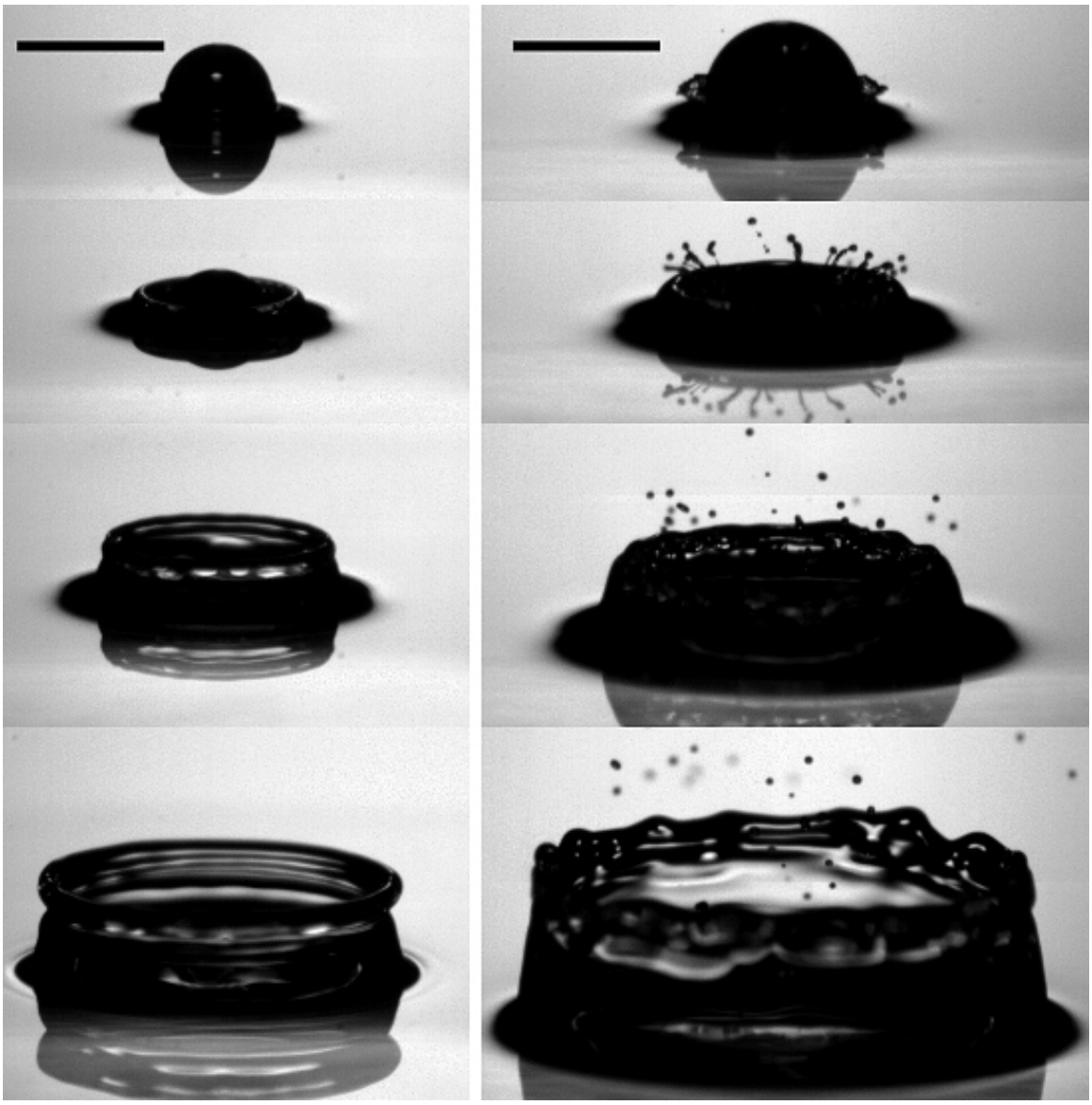

Figure 2.6: Two series of images display the different splashes produced by silicone oil (left) and a water-glycerol mixture (right). Dimensionless numbers for the oil, $Re = 4043$ and $We = 206$, while the water has $Re = 4498$ and $We = 204$. Between the two splashes there is a 10.1% different in Reynolds number and 1.0% difference in Weber number. Pairs of images were recorded at 238, 475, 1045, and 2518$\mu$s after impact. The scale bar indicates a length of 2mm.

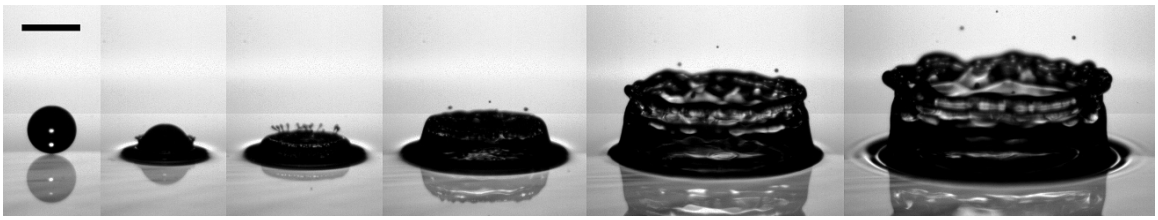

Figure 2.7: The oil does not produce microdroplets until the Reynolds and Weber numbers are significantly higher than the threshold for water. In this series a drop of oil with $Re = 5739$ and $We = 412$ produces a splash very similar to the water (right column) displayed in Figure 2.6

# CHAPTER III

# Fluid Sheets

## 3.1 Introduction

In the previous chapter we demonstrated inconsistencies in the conventional phase portrait used to characterize splashing. These inconsistencies were most pronounced in the high-Reynolds number region. In this chapter, we examine another feature of splashing, the origin and evolution of fluid sheets. We begin by carefully defining the structure of a splash and then present data in hopes of clarifying and extending previous research.

## 3.2 Anatomy of a Splash

It is often difficult to make comparisons among previous research due to a lack of uniformity describing features of a splash. For this reason, our first objective is to carefully define key terms so that there is no confusion about structures that we are observing. Figure 3.1 depicts the splash for times immediately and long after impact.

### 3.2.1 The Ejecta Sheet

We define the time, $t_0 = 0$, to be the point at which the bottom edge of the drop initially makes contact with the layer of fluid. At this point, Howison *et. al.* present a theory for the formation of an *ejecta sheet* [4]. Neglecting the effects of viscosity, surface tension (thus $Re = We = \infty$), and air, their work describes a sheet that instantaneously shoots out horizontally to infinity. The existence of this sheet has been previously proposed by Thoroddsen [9] in experimental data. Weiss and Yarin [10] also find evidence of this sheet in numerical simulations, but show the ability of

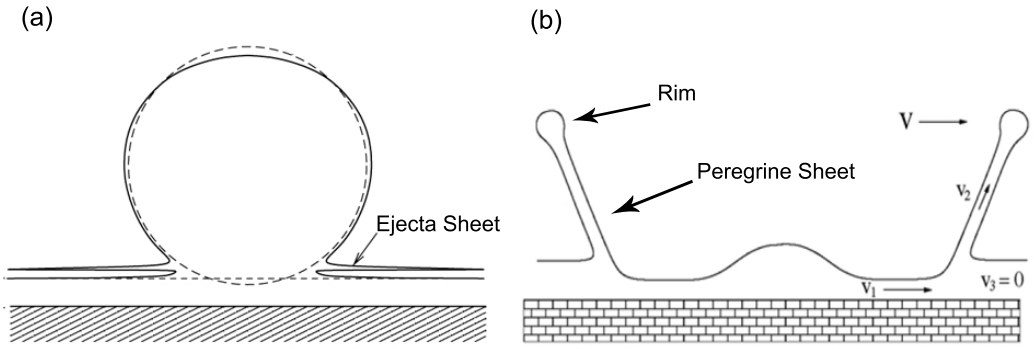


Figure 3.1: (a) Immediately after impact, an ejecta sheet forms, shooting out horizontally. (b) For later times, the Peregrine sheet forms, propagating outward and upward. The rim of this sheet eventually becomes unstable, sharpening into jets that may pinch off into secondary droplets.

surface tension effects to suppress it as the Weber number grows larger. A stylized depiction of the ejecta sheet can be found in Figure 3.1a.

Previous work suggests the ejecta sheet appear for splashes with $We > 40$ and reasonably high $Re$. For the parameter ranges we probe, previous experimental data predicts sheet formation within the first $10\mu$s after impact, propagating at speeds near 100m/s. Photographic evidence of the ejecta sheet can be found in Figure 3.2.

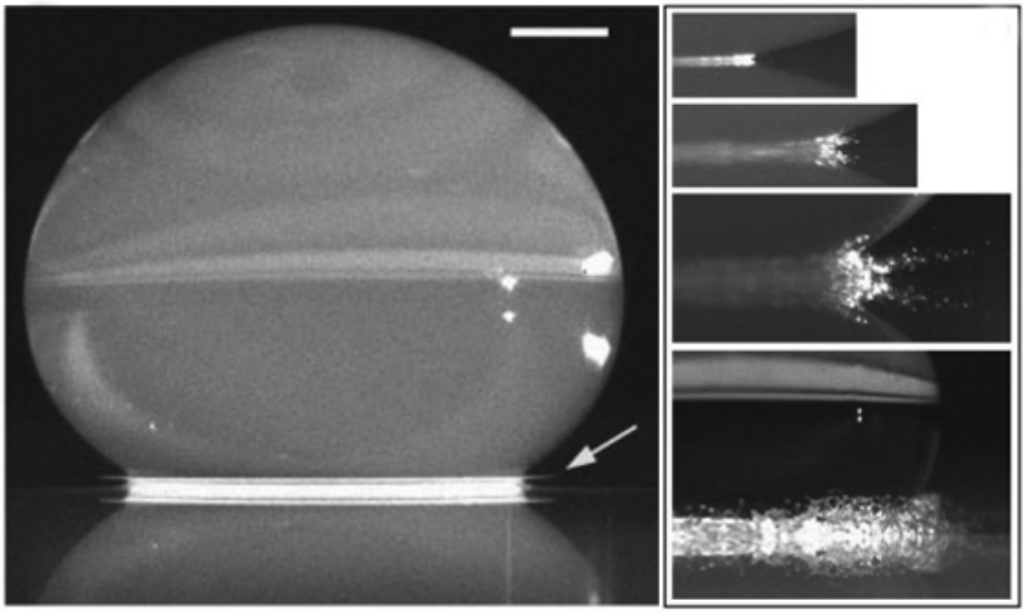

Figure 3.2: The Ejecta sheet, as photographed by Thoroddsen [9], for a water drop with $Re = 4640$ and $We = 2190$.

### 3.2.2 The Peregrine Sheet

After the drop has descended further into the layer, we observe another sheet. We label this sheet the *Peregrine sheet* (though it is sometimes referred to in the literature as the crown sheet) as it was first defined by D. H. Peregrine in 1981 [7]. In his simple model, the drop is treated like a fluid jet impacting onto a thin layer and the resulting fluid flow is analyzed considering conservation laws. These results predict the formation of a fluid sheet flowing outward and upward from the splash center.

The origin and evolution of the Peregrine sheet has been studied in considerable detail. Weiss and Yarin [15] present a theory suggesting a kinematic discontinuity is responsible for the formation of the Peregrine sheet. Though they conclude that the formation and propagation of this sheet is dominated by inertia, further numerical simulations by Weiss and Yarin put bounds on its existence in terms of surface tension and viscosity [10].

As the Peregrine sheet evolves, surface tension acts to pull its leading edge backwards, creating a cylindrical rim at the top of the sheet. In some regimes, this rim becomes unstable, eventually breaking up and jetting into secondary droplets. While the actual mechanism causing this instability is still under debate, Deegan *et. al.* presented compelling evidence pointing to the Rayleigh-Plateau instability. Treating the rim as a cylinder of fluid, surface tension acts to form a series of troughs and crests that may later sharpen to form jets, emitting secondary droplets. For a general summary, Cossali *et. al.* have presented experimental data quantifying the size and speed of the Peregrine sheet's features.

Figure 3.1b shows a cross section of the Peregrine sheet. The formation of this sheet has been found to occur for $We > 40$, becoming unstable and producing secondary droplets for $Re > 1200$. The diameter of the sheet grows in diameter from roughly 5 to 20mm and reaches heights of nearly twice the diameter of the drop over a time span of around 5ms. Two examples of the Peregrine sheet can be seen in Figure 3.3.

### 3.2.3 Relationship Between Ejecta and Peregrine Sheets

The relationship between the ejecta and Peregrine sheets is a major source of ambiguity in current research. In some cases, they are described as two distinct sheets that may or may not interact, while in other cases, it is suggested that one sheet grows into the other. A review of the various theories concerning its creation

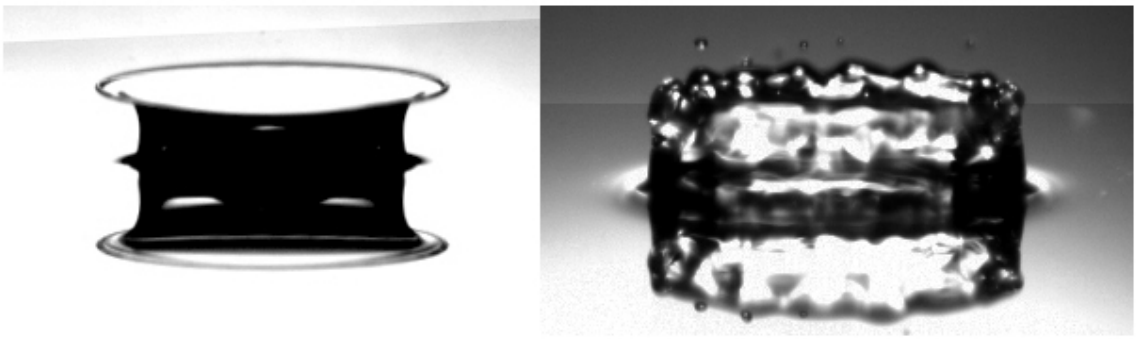

Figure 3.3: Two instances of the Peregrin sheet are shown. The left results from a silicone oil splash for high $We$ number and low $Re$ number while the right is produced by water at low $We$, high $Re$ numbers.

and evolution comes from Deegan *et. al* [2].

The ejecta sheet has been identified as a possible mechanism for microdroplet creation, where the small, fast moving ejecta sheet breaks up, forming secondary droplets. In some regimes, with both a crown splash and microdroplets present, it is thought that the ejecta sheet may ride up the Peregrine sheet, shooting off micrdroplets when it reaches the leading edge. In these splashes, we see the ejection of these microdrops before the Peregrine sheet becomes unstable and pinches off into its own secondary droplets. Finally, Weiss and Yarin [10] have observed, numerically, the case where the ejecta sheet collides with the thin liquid layer and entraps air bubbles.

In previous research, however, it is often unclear which one of these evolutionary paths was observed. Due to differences in the time and length scales of the two sheets, experiments designed to capture one, are generally not continued into the regime of the other. While we do not exaust all possible parameter regimes, we present a series of experiments that aim to explore the origin and evolution of both of these sheets.

## 3.3 Apparatus and Procedure

In addition to the video capturing apparatus depicted in the previous chapter (Figure 2.4), a Canon EOS 20D was used to take still photographs with much higher resolutions so as to capture any small, fast moving sheets. A stacked lens system was used to achieve up to 5 times magnification. For lighting, a 500ns Palflash 501 flash was employed.

Though many macrophotography techniques exist, such as specialized lenses or

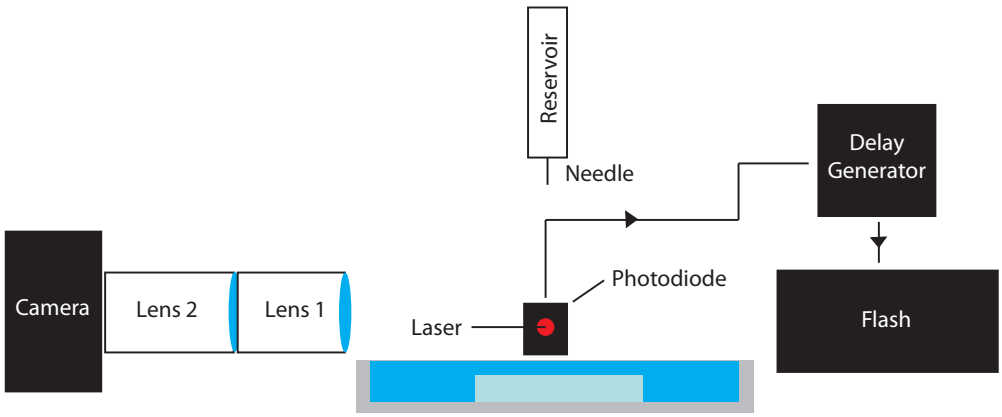


Figure 3.4: Apparatus for collecting data on fluid sheets.

bellows, we used a stacked lens configuration to achieve remarkably high magnification with little distortion. In this configuration we reverse mounted a short focal length (Nikkor 55mm), prime lens, onto the front of a lens with longer focal length (Nikkor 105mm). With the additional use of extenders, our calibrations showed overall magnification of $4.6 - 5.2$ times. A diagram of this apparatus can be found in Figure 3.4.

The price of this added resolution, however, was an extremely small depth of field and short working distance. The depth of field is the thickness of the "in-focus" region of a photograph, while the working distance is the distance from the front of the lens to the in-focus region. With stacked lenses, our working distance was reduced to 1cm, while the depth of field was even smaller ($<$ 1mm). This made it an extremely tedious task to obtain images as drops were required to fall consistently within a 1mm region.

Due to the spatial restrictions placed on the apparatus because of the small depth of field and short working distance, the fluid layer depth could not be accurately controlled. We disregarded this concern, however, because the ejecta sheet forms immediately after impact, before the drop has time to penetrate the layer. Thus, there is little time for the drop to be affected by the presence of a deep pool or shallow layer.

In order to obtain a time series of images, a delay generator was used to time the firing of the flash. A photodiode and laser triggered this sequence. When a falling drop cut the laser beam, a signal was sent to the delay generator, which then sent a signal to the flash. By changing the delay time, images could be obtained in $5 - 10\mu$s intervals.

Using this method, we were able to capture series of incredibly high resolution images of splashing. Coupling these still images with video captures, we were able to obtain a much clearer picture of the features of and relationship between these two liquid sheets.

## 3.4 Results

We first present evidence that the relationship between the two sheets depends on the region of the phase space the splash is in. In some cases, the two sheets are merely one in the same, with the ejecta sheet evolving into the Peregrine sheet. In other cases, there are clearly two sheets, one much smaller and faster than the other.

Both 5cSt silicone oil and pure water were used to capture splashes in two regions of phase space. The oil droplet splashing occur in the high Weber number and low Reynolds number regime, while the water resides in high Reynolds number and low Weber number region. For both splashes, a series of images from less than $10\mu$s after impact until the establishment of the Peregrine sheet (roughly around $> 200\mu$s after impact) was captured.

In both cases, we see a small sheet formed just after impact. This sheet, however, remains very close to the surface of the drop. Despite these similarities, its evolution is radically different for different fluids. We capture video for the water droplet at sixty thousand frames-per-second, roughly one image every $16\mu$s. Figure 3.5 shows two distinct sheets. The first, appears less than $10\mu$s after impact and climbs upward, hugging the surface of the drop. This small sheet eventually becomes unstable, pinching off into microdroplets characteristic of splashes in this portion of phase space.

Taking a closer look at the initial stages of the ejecta sheet, we use high resolution still photographs to examine times between 5 and $200\mu$s after impact. These photographs confirm the existence of a small, fast moving sheet that breaks up to create microdroplets (Figure 3.6). To reduce the turbulence and noise seen in these splashes, we study impacts of water for lower velocities. In these images (Figure 3.7), we observe the ejecta sheet riding up the surface of the impacting drop.

After the ejecta sheet has become unstable (roughly $200\mu$s after impact), the Peregrine sheet emerges. This sheet grows upward and outward, appearing slightly separated from the impacting drop. The Peregrine sheet eventually develops its own instability, possibly jetting into secondary droplets during a crown splash.

We also examine a drop of 5cSt silicone oil on a thin layer of fluid. In contrast to

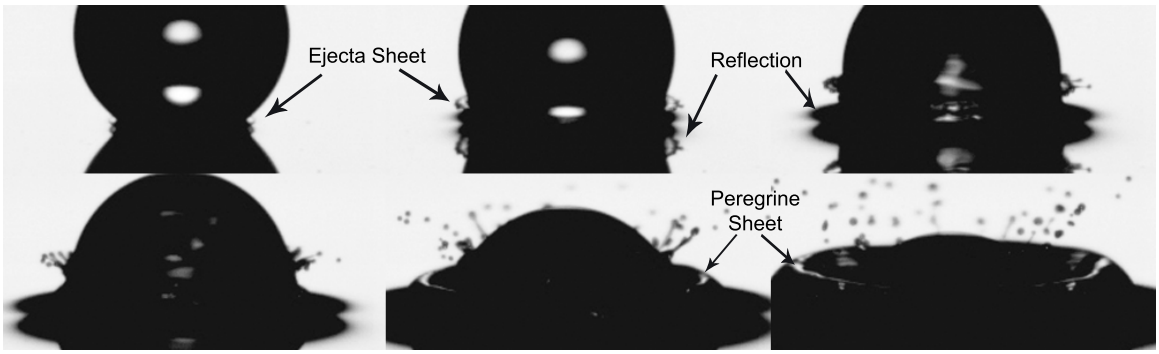


Figure 3.5: A water drop ($Re = 4498$, $We = 204$) in the first moments after impact. Images correspond to times of 47, 78, 110, 173, 236, 378, 488$\mu$s after impact. The sheet is seen first, breaking up into microdroplets just as the Peregrine sheet begins to form. We are careful to distinguish between splash features and reflections or other optical distortions.ill

water, this splash takes place in an entirely different portion of phase space, having high Weber number and low Reynolds number. We still find small, fast moving sheet emerging just after impact, but this time, we cannot distinguish it from the Peregrine sheet (Figure 3.8). This sheet neither becomes unstable nor produces microdroplets, but continues growing upward and outward away from the surface of the drop.

From these experiments, we conclude that there is no single relationship between the ejecta sheets and Peregrine sheet. In some cases, one sheet originates shortly after impact, becoming unstable in its early stages, followed by the emergence of a second sheet, while in others, the sheets are one in the same.

## 3.5 Conclusion

Through this series of experiments, we hope to have clarified the possible relationships between two fluid sheets that emerge during splashing. For high Reynolds number, low Weber number splashes, we see two unique sheets. The first (ejecta sheet) appears immediately after impact, becoming unstable and breaking up to create microdroplets, while the second (Peregrine sheet), develops into the familiar crown splash. For splashes with high Weber numbers and low Reynolds numbers, however, we find no visible indication of two unique sheets. The single sheet that develops just after impact does not show an early instability and grows continuously, eventually becoming what is referred to as the Peregrine sheet.

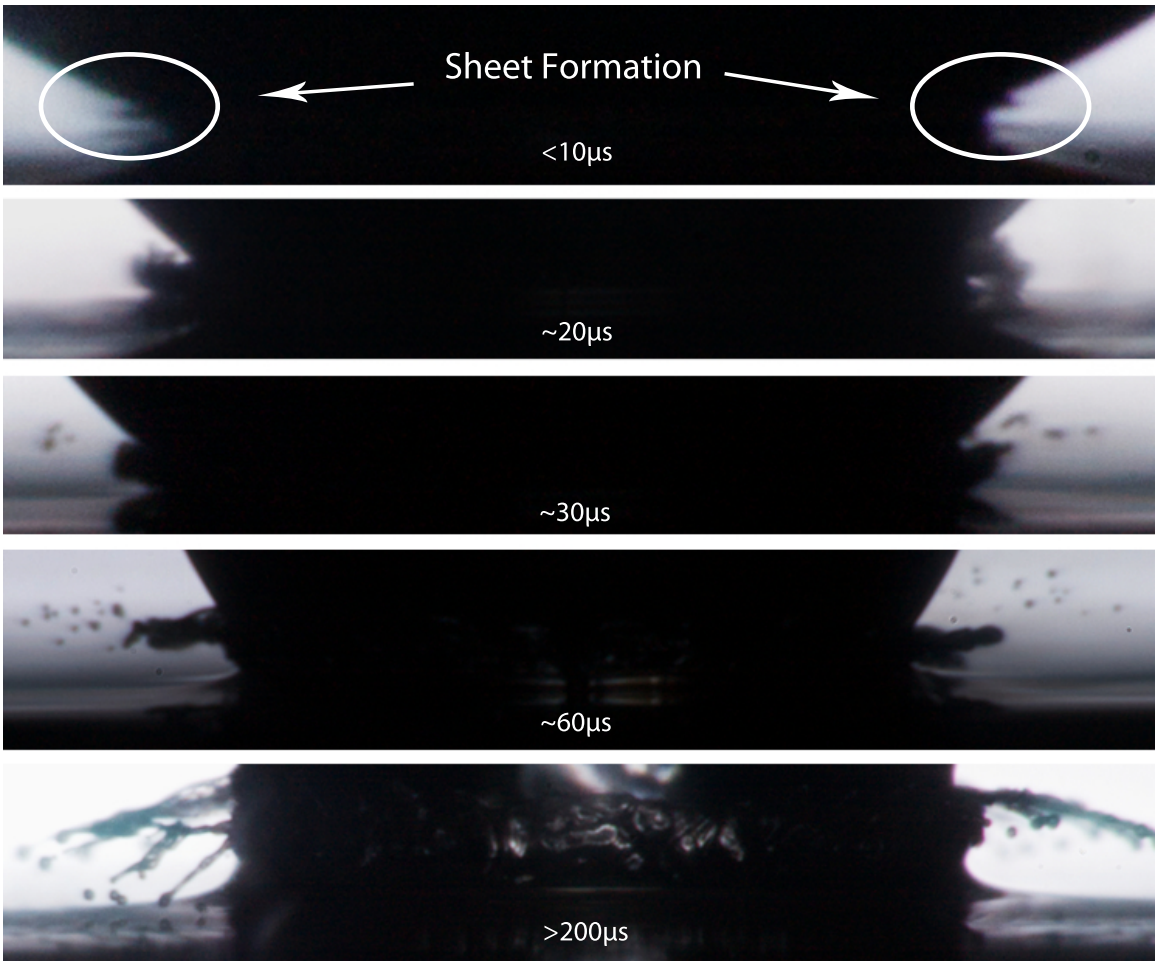


Figure 3.6: A water droplet ($Re = 5500$, $We = 200$) impacting on a thin layer of fluid. Again, only one sheet is seen. Directly after impact, this sheet develops an instability, producing microdroplets characteristic of splashing in this regime. This same sheet then evolves into the Peregrine sheet and breaks up once again into larger, secondary droplets.

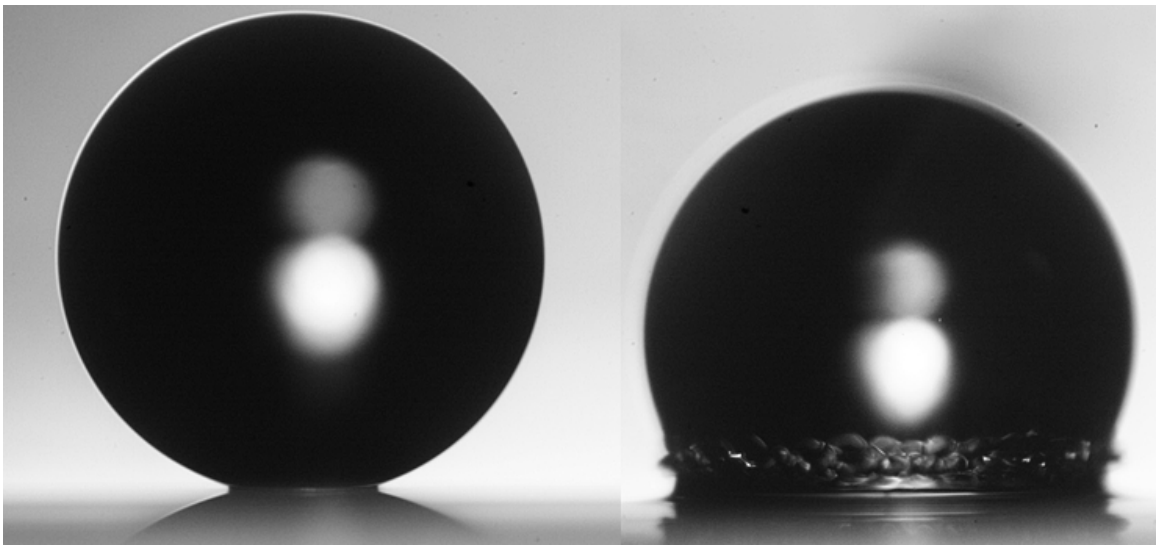

Figure 3.7: A water drop with low impact velocity. A very unstable sheet of fluid is observed riding up the surface of the drop.

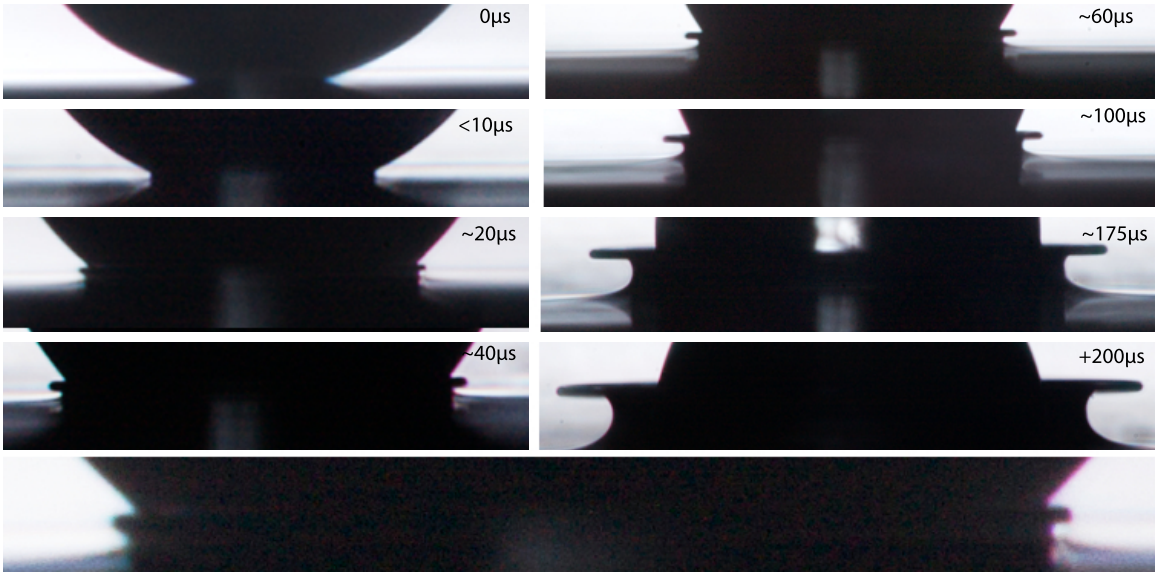


Figure 3.8: A series of images tacking the evolution of the sheet produced by a 5cSt oil droplet with $Re = 699$ and $We = 426$ impacting on a thin layer of fluid. We find that there is only one sheet that develops shortly after impact, eventually growing into the Peregrine sheet.

# CHAPTER IV

# The Effects of Surrounding Gas on Splashes

## 4.1 Introduction

In previous chapters we have presented a series of experiments detailing qualitative differences between splashes and their features. These differences contradict various theoretic assumptions such as dynamic similarity and demonstrate a need to revise stylized models of splashing. We are left to seek new explanations for these findings.

The most obvious omission in most models and experiments is the influence of the surrounding gas on a splash. For any given splash, there are a number of parameters that cannot be controlled for. We consider oscillations or circulation in the drop as the result of pinching off the needle, friction forces from contact with the air, or bubbles that may become trapped during the splash itself. Furthermore, we suspect the small, fast-moving fluid sheets may have very non-trivial interactions with the gas. To explore these possibilities, we conduct a series of experiments whereby the gas in which the splash occurs is varied.

## 4.2 Previous Work

Though interactions with the surrounding gas are almost completely ignored in the literature involving fluid on fluid splashing, recent work has been done studying the affects of air in splashes on dry surfaces. Both numerical simulation and experiments reveal an intimate connection between air and splash.

The first evidence of this relationship was presented by Xu *et. al* in a series of experiments where both the composition and pressure of the surrounding gas were varied for splashes on a smooth dry surface [13]. These experiments show a threshold pressure below which no splashing observed. Amazingly, the entire crown splash can

be suppressed simply by removing the surrounding gas. Splashes for various pressures can be found in Figure 4.1.

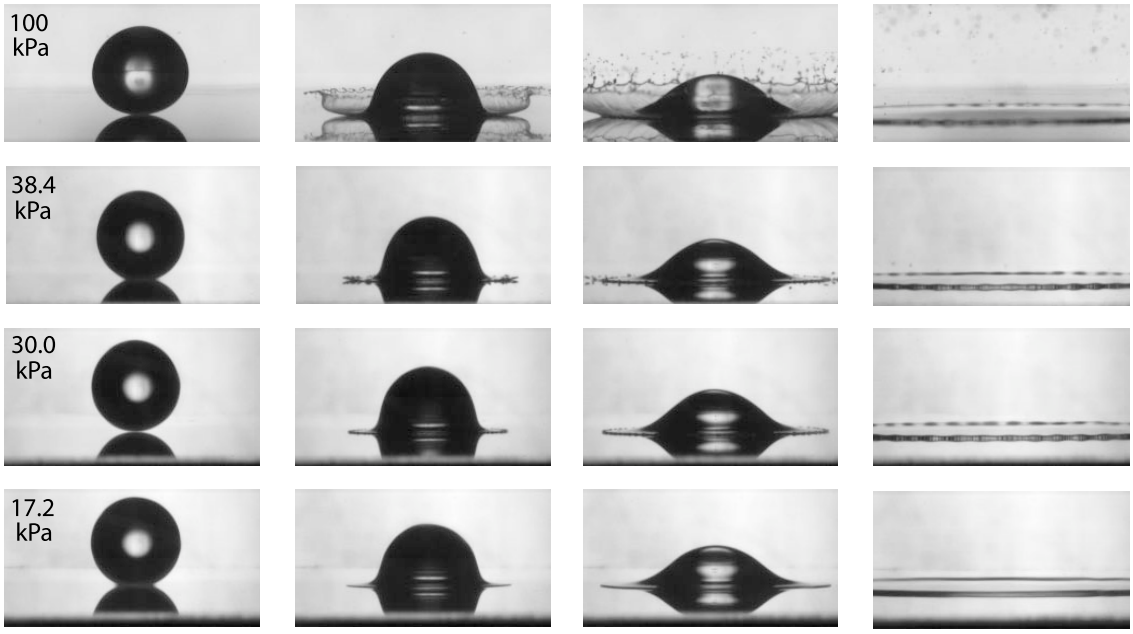


Figure 4.1: An alcohol drop is photographed as it splashes on a smooth dry surface for various pressures of the surrounding gas. For low enough pressures, the splash is completely suppressed and the drop spreads evenly over the surface [13].

Furthermore, Xu *et. al* found that this threshold pressure is different for different gases. For experiments in air, helium, krypton, and $SF_6$, helium had the highest threshold pressure, while $SF_6$ had the lowest. Their results suggest that the vertical component of the fluid sheet's velocity is determined by interaction between the liquid and the air. As the drop impacts, fluid is initially ejected horizontally where it collides with the surrounding gas, when the pressure of this gas or the speed of the sheet is great enough, the fluid sheet lifts off the surface, riding the air upwards.

More recent work by Xu *et. al.* reveals another control parameter for splashes on dry surfaces. Using vacuum to control for the existence of the crown sheet, surface roughness was varied, revealing a mechanism for a different type of splash. Even for pressures below the threshold for splash suppression on smooth dry surface, splashing still occurred on rough surfaces. These splashes, labeled "prompt splashes", are characterized by the immediate break up of the liquid sheet into smaller droplets (Figure 4.2) [12].

While the boundary conditions for fluid on fluid splashes are undoubtedly different

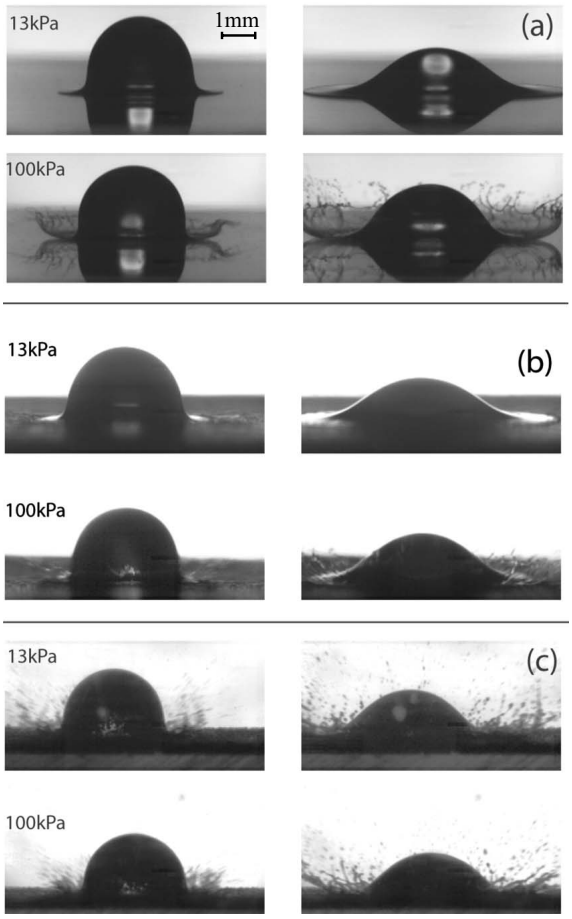


Figure 4.2: A drop is photographed splashing on a dry, solid surface for various pressures and surface roughnesses. Splashes on smooth surfaces (a), are completely suppressed by lowering the gas pressure. For rougher surfaces (b and c), a different type of splash, characterized by immediate breakup of the fluid sheet into microdroplets, is seen. This second type of splash persists despite changes in pressure [13].

from those in fluid on solid splashes, we cannot help but the see the analogy between these two district splashes in vacuum and the microdroplet and crown splashes from previous chapters. This work motivates us to look at the surrounding gas as a parameter that may resolve discrepancies in our current phase portrait.

## 4.3 Apparatus and Procedure

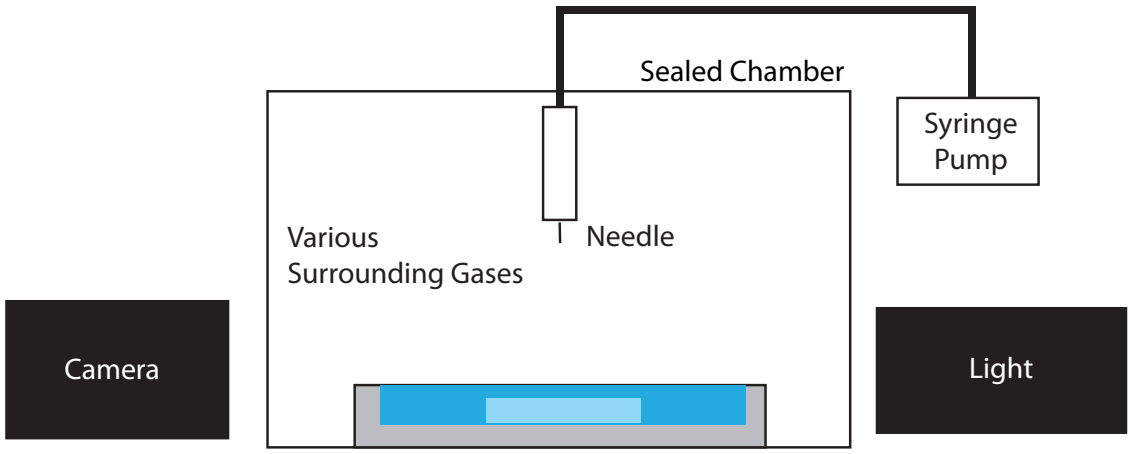


Figure 4.3: A high-speed video capture setup and a custom built sealed chamber was used to capture images of splashing for various surrounding gases.

For these experiments, the high-speed video setup used in previous experiments was employed. A sealed chamber was constructed from clear plastics so that the air could be pumped out and replaced with either helium or $SF_6$. This chamber was not constructed to hold vacuum, thus the air was pumped out at roughly the same rate that the new gas was pumped in.

Helium and $SF_6$ were chosen to test gases both more and less dense than air. Helium, roughly seven times less dense than air, displayed the highest threshold pressure in experiments by Xu *et. al.*, making it the most likely candidate to alter a splash despite the fact that we were not operating under vacuum. $SF_6$, being five times denser than air, was chosen to complement helium. Both of these gases are inert and relatively easy to procure.

To ensure that the chamber was sufficiently full of helium, we filled a balloon with helium and released it to float to the top of the chamber. We then went about replacing the air with helium and the balloon begins to descend. When the balloon

had reached the bottom of the chamber, we sealed the valves and begin taking measurements. In this case, because the chamber cannot be opened to re-fill the drop reservoir, we use a syringe pump to control the drop rate. A similar procedure was used for $SF_6$.

## 4.4 Results

For a given drop height, we find that replacing the surrounding gas changes only the droplet's impact speed (different drag coefficients) and has no affect on splash characteristics. Comparing drops in different gases, all with the same impact speed, reveals identical splashes, suggesting that interactions between the drops and the surround air are indeed negligible as the literature assumes.

We find that both water-glycerol mixtures as well as 0.65cSt silicon oil produce splashes that are qualitatively identical in all three gases, helium, $SF_6$, and air. Furthermore, we find that, for each fluid, the transition to splashes with microdroplets occurs at the same fluid specific $Re$ and $We$ numbers in all three gases. Finally, we again find that splashes of oil and splashes of water glycerol display vast differences despite being close in phase space.

Figure 4.4 shows three splashes, one for each of the three surrounding gases. All three splashes have high $Re$ number ($\approx 5000$) and low $We$ number ($\approx 300$). Each splash displays the microdroplets and all fluid sheets evolve in a similar fashion. The number and size of the microdroplets may seem to vary, but these qualities are almost never consistent between splashes due to many small perturbations that undoubtedly affect initial conditions.

## 4.5 Conclusion

Despite an intimate connection between the surrounding gas and splashing for droplet impacts on a solid surface, we find no evidence that liquid on liquid splashes are affected by changes in gas composition. This result affirms theoretic assumptions and suggests ignoring the effects of air in formal models is justified. It is somewhat unsatisfactory, however, that we have not found an explanation for discrepancies in our phase space. We find these problems persist despite changing this variable.

While our experiments varied only composition, and not pressure of the surrounding gas, previous work suggests that helium should have affected splashing if interaction was occurring. Thus we are left to reconsider the mechanism that may explain

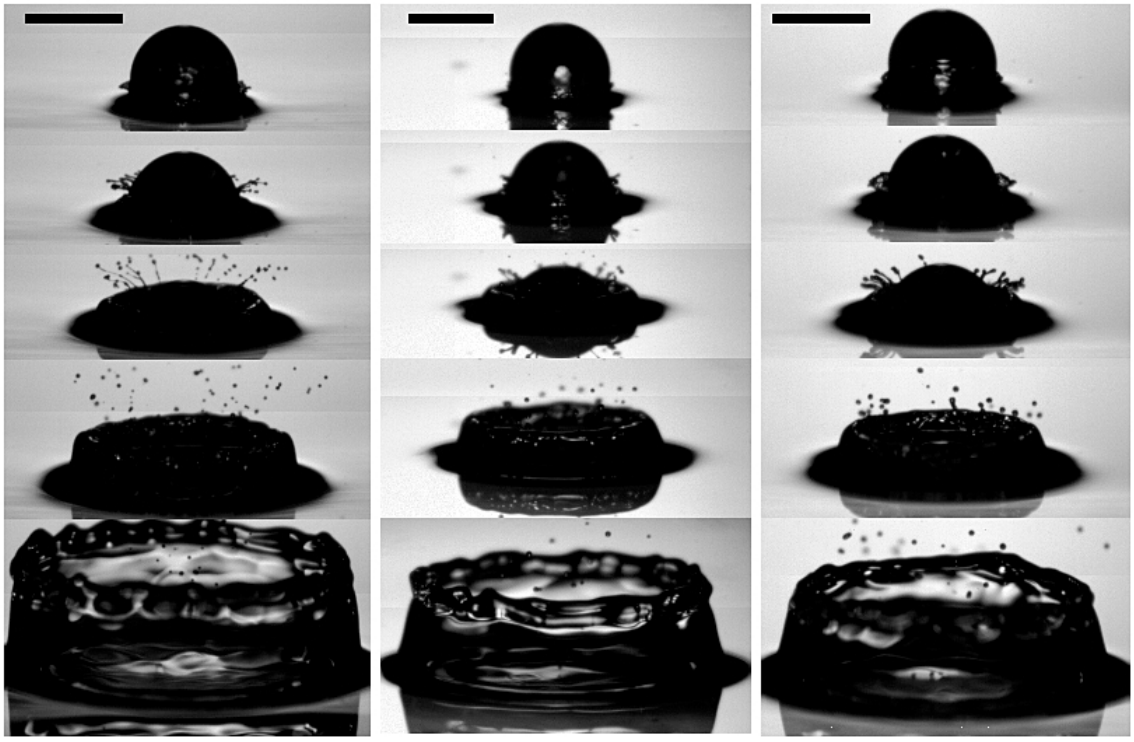

Figure 4.4: Three splashes are captured for three different surrounding gases. Helium (left), $SF_6$ (center), and air (right), all produce qualitatively similar splashes. Images were taken at 143, 238, 380, 665, and 1800$\mu$s after impact. All three splashes have $Re \approx 5000$ and $We \approx 300$.

the qualitative differences exposed in previous chapters. Alternative explanations for phase space discontinuities may be fluid circulation in the drops due to air drag or bubble entrapment during impact.

# CHAPTER V

# Miscellaneous Experiments with Splashes

## 5.1 Introduction

Finally, we present a series of experiments exploring the many permutations of initial conditions of splashes. We study fluid on fluid splashes where the two fluids are entirely different (such as oil on water) as well as solid on fluid impacts, dropping small metal spheres onto thin fluid layers. While the parameters of experiments are not as precisely controlled as in previous chapters, many interesting questions are raised. We hope to at least provide insight into several interesting mechanisms

## 5.2 Solid on Fluid Impacts

In addition to fluid on fluid splashing, we also perform experiments involving solids splashing on a thin layer. These experiments seek to verify numerical simulations done by Weiss and Yarin [10] and Josserand *et. al.* [5] that suggest the fluid sheet generated in splashing is composed of fluid from both the layer and the drop.

We use an experimental set up similar to the one used to study the fluid sheets generated during a splash as explained in Chapter III. Instead of a liquid drop impacting on a thin layer of fluid, we use small metal spheres of varying sizes. In most cases, spheres with a diameter of 2mm were used, matching the diameter of water droplets.

Figure 5.1 shows two stainless steel spheres impacting on a thin layer of water, one sphere has been cleaned thoroughly, while the other was coated with a hydrophilic substance. The spheres were dropped from a height of 40cm and impacted with roughly the same velocity as water dropped from the same height. In these splashes, we find that fluid sheets evolve in a similar way to those of fluid on fluid splashes. There is a small, fast moving initial sheet that hugs the side of the impacting object.

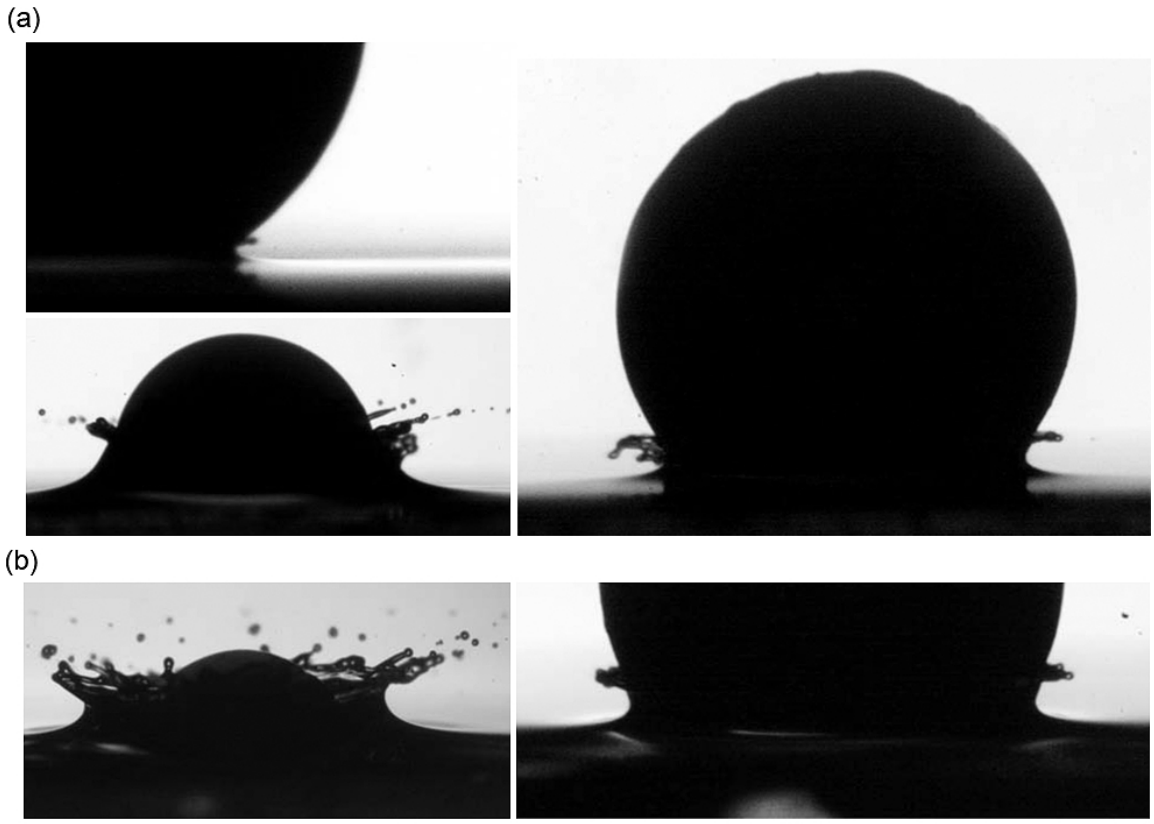


Figure 5.1: Solid, stainless steel spheres impact on a thin layer of water. Both clean (a) and coated (b) spheres produce identical splashes. These splashes feature small, fast moving fluid sheets similar to those found in water on water impacts.

This sheet becomes unstable and pinches off into jets, forming microdroplets. Unlike the water on water splashes, we do not find two separate sheets. Instead, we see the Peregrine sheet evolving from the initial sheet eventually becoming an unstable crown.

Because the impacting object contributes no fluid to the splash and the layer depth is not controlled ($H \approx .5$), it is difficult to conclude much from these qualitative differences. This analysis may suggest, however, that the fluid in the drop contributes significantly to the formation and propagation of the Peregrine sheet. Finally, we note that the presence of a hydrophilic substance coating the sphere has no visible effect on the evolution of the splash.

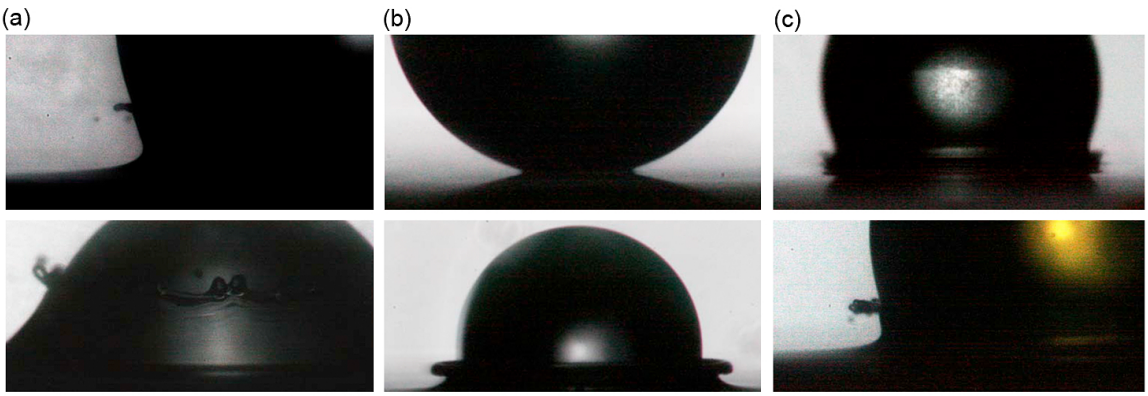


Figure 5.2: Three different combinations of fluid, (a) pure glycerin on water, (b) silicone oil on water, and (c) thick motor oil on water, are studied. The more viscous impacting fluids, glycerin and motor oil (a and c) produce splashes similar to the solid on liquid experiments, while the silicone oil on water feature a smooth, stable Peregrine sheet resembling that found in oil on oil splashes.

## 5.3 Differing Fluids

In addition to solids impacting on liquids, we examine splashes produced in liquid on liquid impacts, but where the impacting drop and thin layer are composed of different fluids. We test study three cases, the first is pure glycerin impacting on water, the second, silicone oil on water, and the third, a thick motor oil on water. In all three cases, drops were released from a syringe at a height of 40cm from a thin layer of water, again ensuring impact velocities near those studied in previous chapters. Images from each of these cases can be found in Figure 5.2.

Pure glycerin, more viscous than water, produces a splash much like that of a solid sphere impacting on water. A small fluid sheet rides the surface of the drop, eventually becoming unstable. We find a larger, separate Peregrine sheet as in the case of water on water splashes. This may suggest that the formation and evolution of the Peregrine sheet is related to the viscosity of the impacting object.

For silicone oil on impacting water, we find, somewhat surprisingly, that the splash is qualitatively similar to that of oil on oil splashes. No initial ejecta sheet is formed, but instead the Peregrine sheet evolves upward and outward from the impact point. No microdroplets are present. It is interesting that the Peregrine sheet is very smooth and stable, nearly identical to that in oil on oil splashes. Despite the thin layer being composed of pure water (which we have seen produces unstable fluid sheets and microdroplets), there does not seem to be any evidence of its influence.

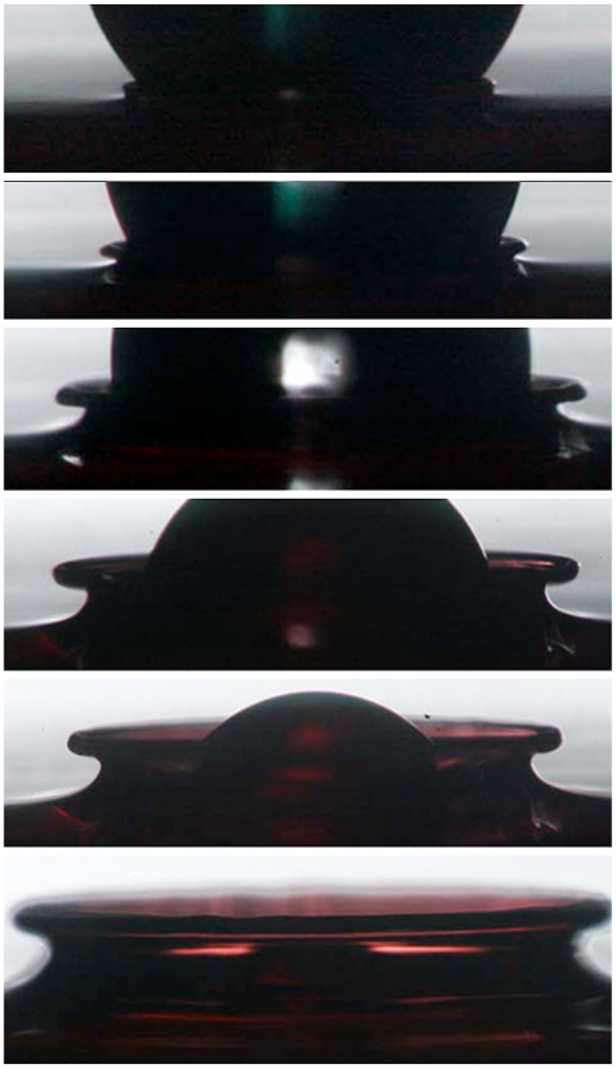

Figure 5.3: For silicone oil impacting on a thin layer of water, we introduce red dye into the liquid layer in an attempt to better understand the composition of the fluid sheet produced. Despite the sheets similarity to the oil sheet produced in oil on oil splashes, its red color suggests at least some of the fluid comes from the layer.

In addition to the low viscosity silicone oil, we drop a very thick, viscous motor oil into a thin layer of water. Much like the glycerin drop impacting on water, we find that the splash is qualitatively similar to that of the solid sphere. A small fluid sheet hugs the drop's surface, quickly becoming unstable. This result adds weight to our intuition that the viscosity of the drop fluid plays some role in the qualitative features of a splash.

## 5.4 Sheet Composition

Finally, we seek to explore contributions from drop and thin layer to the fluid sheet(s) produced during splashing. We again drop low viscosity silicone oil on a thin layer of water, this time introducing red dye into the layer. Figure 5.3 shows a time series of a splash. As noted in the previous section, the oil on water splash produces

a smooth, stable Peregrine sheet, similar to that found in oil on oil splashes. From the images, we can clearly see the clear drop impacting on the red layer.

As the sheet grows, we see that there is a pronounced red tint to the Peregrine sheet, suggesting that at least some of the sheet's fluid comes from the thin layer of water. This result is surprising because the sheets characteristics suggest it is mostly oil, while its color suggests water may be present. By pure conjecture, we wonder if this effect is due to some coating process where the oil from the drop acts a thin membrane for the water in the Peregrine sheet. We are reminded of Ben Franklin's famous party trick whereby he was known to calm an entire pond by releasing a small teaspoon of oil to coat the water [3].

## 5.5 Conclusion

In this chapter, we have presented a series of exploratory experiments. Though perhaps these results raise more questions than they answer, we hope they provide insight and intuition into combinations of system parameters yet to be studied. We find both similarities and differences for splashes produced by solid on liquid impacts. Splashing involving two different liquids reveal a possible relationship between viscosity of the features of a splash, while further study reveals new information regarding the composition of fluid sheets.

# CHAPTER VI

# Conclusion

In this work, we have presented a suite of experiments studying the complexities of splashing. Using both video and still imaging techniques, we have explored a range of initial conditions and system parameters in hopes of better understanding the origin and evolution of splashing. Though current work and theoretical models have made progress in capturing many fundamental parameters, we find that the phase space described in these models is still incomplete. Our experiments reveal that two splashes, described by the same dimensionless quantities, can demonstrate qualitatively distinct features. These findings suggests that the set of equations and parameters currently used to describe a splash remain incomplete.

In an attempt to find the source of these discrepancies, we began by clarifying the anatomy of a splash, combining and translating many terms and features described in previous work. Having constructed a universal language, we examined the origin and evolution of fluid sheets produced during a splash in the hope that they might be a point of divergence explaining the phase portrait inconsistencies. Here we found that these small, fast moving, and often unstable sheets were indeed sensitive to fluid parameters, and the source of many splash features such as microdropets and crowns.

Having established the importance of the propagation of these fluid sheets, we attempted to uncover control parameters in their evolution. Building on work done in similar experiments involving liquid drops impacting on dry, smooth surfaces, we studied the importance of the surrounding gas in liquid on liquid splashes. Unlike the case of splashing on a dry surface, we found that changing the composition of the gas does not have any affect on the splash. These experiments suggest that theoretical models are indeed justified in neglecting the effects of air in models. Unfortunately, these findings also left us without a satisfying explanation of phase portrait discrepancies.

Finally, we detailed various miscellaneous experiments designed to explore other combinations of splashing parameters not considered in the literature. Solid spheres impacting on a thin layer of water were found to produce microdroplets and fluid sheets similar to those found in water on water splashes, while splashes involving two different liquids produced varied results. Impacting drops with high viscosity lead to splashes qualitatively similar to those of solids impacting on liquid, while low viscosity silicone oil splashing on water produced features seen in oil on oil splashes. In other experiments, we explored the fluid composition of the fluid sheets present silicone oil impacts on water. Despite the fluid sheet displaying characteristics of oil on oil splashes, there is at least some fluid contribution from the water layer. Though these miscellaneous experiments are somewhat less controlled and precise, we hope they raise interesting questions and provide some insight into splashing mechanisms.

While much of this work has been qualitative in nature, given the complex fluid dynamics of a splash, these types of experiments are invaluable, providing motivation and direction for more theoretic and quantitative pursuits. While we do not specifically consider applications of this work, these results may aid the process of choosing correct system parameters in order to achieve certain splashing characteristics. Finally, we hope that the phenomenon of splashing can at least be appreciated for its aesthetic quality and beauty.

# BIBLIOGRAPHY

# BIBLIOGRAPHY


[1] G. E. Cossali, M. Marengo, A. Coghe, and S. Zhdanov. The role of time in single drop splash on thin film. *Experiments in Fluids*, 36(6):888–900, June 2004.

[2] R D Deegan, P Brunet, and J Eggers. Complexities of splashing. *Nonlinearity*, 21(1):C1–C11, 2008.

[3] Benjamin Franklin, William Brownrigg, and Farish. Of the stilling of waves by means of oil. extracted from sundry letters between benjamin franklin, ll. d. f. r. s. william brownrigg, m. d. f. r. s. and the reverend mr. farish. *Philosophical Transactions (1683-1775)*, 64:445–460, 1774.

[4] S. D. Howison, J. R. Ockendon, J. M. Oliver, R. Purvis, and F. T. Smith. Droplet impact on a thin fluid layer. *Journal of Fluid Mechanics*, 542(-1):1–23, 2005.

[5] Christophe Josserand and Stéphane Zaleski. Droplet splashing on a thin liquid film. *Physics of Fluids*, 15(6):1650–1657, 2003.

[6] C. Mundo. Droplet-wall collisions: Experimental studies of the deformation and breakup process. *International Journal of Multiphase Flow*, 21(2):151–173, April 1995.

[7] D. H. Peregrine. The fascination of fluid mechanics. *Journal of Fluid Mechanics Digital Archive*, 106(-1):59–80, 1981.

[8] C. D. Stow and M. G. Hadfield. An experimental investigation of fluid flow resulting from the impact of a water drop with an unyielding dry surface. *Proceedings of the Royal Society of London. Series A, Mathematical and Physical Sciences*, 373(1755):419–441, 1981.

[9] S. T. Thoroddsen. The ejecta sheet generated by the impact of a drop. *Journal of Fluid Mechanics*, 451(-1):373–381, 2002.

[10] Daniel A. Weiss and Alexander L. Yarin. Single drop impact onto liquid films: neck distortion, jetting, tiny bubble entrainment, and crown formation. *Journal of Fluid Mechanics*, 385(-1):229–254, 1999.

[11] A. M. Worthington. *A Study of Splashes*. Longmans, Green, and Co., 1908.

[12] Lei Xu, Loreto Barcos, and Sidney R. Nagel. Splashing of liquids: Interplay of surface roughness with surrounding gas. *Physical Review E*, 76(6):066311+, Dec 2007.

[13] Lei Xu, Wendy W. Zhang, and Sidney R. Nagel. Drop splashing on a dry smooth surface. *Physical Review Letters*, 94(18):184505+, May 2005.

[14] A. L. Yarin. Drop impact dynamics: Splashing, spreading, receding, bouncing. *Annual Review of Fluid Mechanics*, 38(1):159–192, January 2006.

[15] A. L. Yarin and D. A. Weiss. Impact of drops on solid surfaces: self-similar capillary waves, and splashing as a new type of kinematic discontinuity. *Journal of Fluid Mechanics Digital Archive*, 283(-1):141–173, 1995.